Front. Energy 2019, 13(3): 597–602
https://doi.org/10.1007/s11708-018-0576-9

COMMUNICATION

Lijun WU, Yu ZHANG, Bingjiang LI, Pengxiang WANG, Lishuang FAN, Naiqing ZHANG, Kening SUN

Fabrication of layered structure VS_4 anchor in 3D graphene aerogels as a new cathode material for lithium ion batteries

Abstract VS_4 has gained more and more attention for its high theoretical capacity (449 mAh/g with $3e^-$ transfer) in lithium ion batteries (LIBs). Herein, a layered structure VS_4 anchored in graphene aerogels is prepared and first reported as cathode material for LIBs. VS_4@GAs composite exhibits an exceptional high initial reversible capacity (511 mAh/g), an excellent high-rate capability (191 mAh/g at the 5 C), and an excellent cyclic stability (239 mAh/g after 15 cycles).

Keywords VS_4, graphene aerogels, cathode, lithium storage

1 Introduction

With the ever-increasing electronics industry, it is of critical importance to improve the energy storage capability of current batteries by using various strategies. Because of their high energy density, good safety, long cycle life, and less pollution, LIBs have achieved great success in the past decades and have been widely integrated into portable electronics, hybrid electric vehicles, smart grids, and so on attributed to the highly efficient energy storage devices [1]. The conventional cathode, $LiCoO_2$, and $LiFePO_4$ with a practical capacity of 140 and 170 mAh/g and a poor rate capability, are harder to satisfy the actual requirements for the next generation cathode.

Furthermore, with the rapid development of cathode materials with high capacities, transition-metal oxide and fluoride like V_2O_5 [2,3] and FeF_3 [4,5] have received wide attention. These intercalation/deintercalation type cathode electrode materials often display a higher capacity than traditional cathode materials. Recently, research on transition metal sulfides has increased due to their high conductivity, good chemical durability and low cost, and they have been applied in various field such as light harvesting [6,7], catalysis [8,9] and energy storage [10–13]. As a transition-metal sulfide, VS_4 possesses a unique loose stacked framework structure because the chains are connected through weak van der Waals force [14,15]. The large open channels in the loose stacked framework structure provide plenty of sites for Li^+ diffusion and lithiation [16–18].

Although monoclinic VS_4 has been reported as an anode material for LIBs [14,19,20], it is rarely studied as a cathode material for LIBs owing to its complex property in the high electrochemical potential range and the difficulty of preparing pure VS_4 phase. Therefore, the investigation of VS_4 as a cathode material for LIBs is desirable and urgent. The energy storage principle of VS_4 cathode can be expressed as

$$VS_4 + xLi^+ + xe^- \rightleftharpoons Li_xVS_4$$

VS_4 has attracted great interest for its rich resources, low cost, and high theoretical capacity (449 mAh/g with $3e^-$ transfer and 1196 mAh/g with $5e^-$ transfer) which is much higher than the current commercial cathodes, such as $LiCoO_2$ (~140 mAh/g) and $LiFePO_4$ (~170 mAh/g). Despite these merits, the slow Li^+ diffusion and low electrical conductivity of bulk VS_4 have restricted its application in LIBs [19,21]. Therefore, designing and constructing VS_4-based materials with a higher conductivity for LIBs are urgent for developing the next generation LIBs.

Fabricating nanocomposite with carbon materials has been demonstrated as an effective strategy to enhance the conductivity and rate capability of electrode materials, and numerous kinds of carbon materials have been applied

Received Apr. 8, 2018; accepted May 20, 2018; online Sep. 20, 2018

Lijun WU, Yu ZHANG, Bingjiang LI, Pengxiang WANG
State Key Laboratory of Urban Water Resource and Environment, School of Chemistry and Chemical Engineering, Harbin Institute of Technology, Harbin 150001, China

Lishuang FAN, Naiqing ZHANG (✉), Kening SUN (✉)
State Key Laboratory of Urban Water Resource and Environment, School of Chemistry and Chemical Engineering; Academy of Fundamental and Interdisciplinary Sciences, Harbin Institute of Technology, Harbin 150001, China
E-mails: fanlsh@hit.edu.cn; znqmww@163.com

[5,22–24]. Compared with carbon nanotubes (CNTs), graphene possesses outstanding mechanical strength and electrical conductivity due to its unique two-dimensional monolayer structure [25–27]. The high surface area provides graphene with a low fabricating cost and a better interfacial contact compared to CNTs. Moreover, 3D graphene aerogels (GAs) with unique characteristics including a high surface area, a tunable porosity, and large pore volumes, have shown potential applications in the fields of energy storage [10,26,28], catalysis [29], electronic devices and so on. Thus, GAs could be ideal materials to hybridize with VS_4.

In this work, a tactful hydrothermal method is applied to *in situ* synthesize VS_4@GAs hybrid nanostructures for the purpose of improving the rate capability. It is first reported as a cathode material for LIBs. Benefiting from the electron transfer highways and abundant pores for Li^+ diffusion in graphene, the VS_4@GAs hybrid exhibits an enhanced cycle performance and rate capability. A high discharge capacity of 239 mAh/g can be remained after 15 cycles at a current density of 40 mA/g. Even at a high rate of 2000 mA/g, a discharge capacity of 191 mAh/g still can be obtained.

2 Results and discussion

As illustrated in the synthesis strategy toward the VS_4@GAs electrode (Fig. 1), according to the spread growth mechanism induced by electrostatic interaction, VS_4 nanoparticles were homogeneously dispersed on graphene. During the hydrothermal process, C_2H_5NS (TAA) not only serves as a sulfur source to form VS_4, but also acts as a reducing agent to reduce GO to rGO partially. The photos of VS_4@GAs are exhibited in Electronic Supplementary Material (Fig. S1), which reveals a typical graphene aerogels. To confirm the crystal structure and composition of the prepared VS_4@GAs, the X-ray diffraction pattern (XRD) measurement was performed (Fig. S2 in Electronic Supplementary Material). The XRD pattern of the prepared VS_4@GAs has a typical body-centered monoclinic VS_4 phase (JCPDS No. 87-0603). There are not any peaks of other phases in the XRD pattern, indicating the high phase purity of VS_4@GAs.

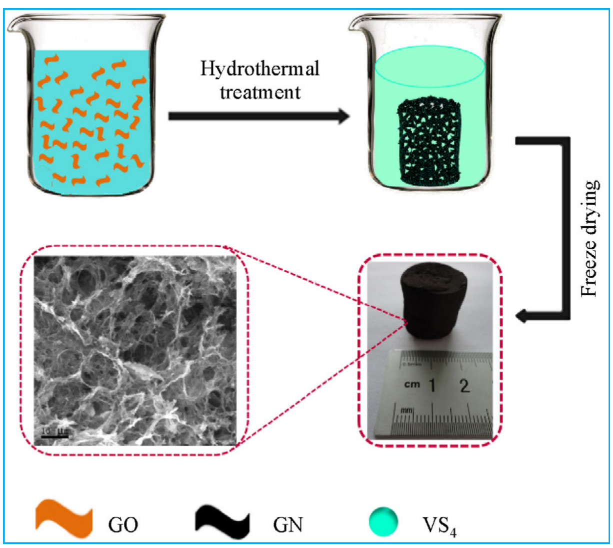

Fig. 1 Schematic diagram of the construction of 3D VS_4@GAs

The microstructure and morphology of the VS_4@GAs were investigated by using transmission electron microscopy (TEM) and scanning electron microscopy (SEM). As shown in Fig. 2(a), the graphene sheets are obviously crumpled. As shown in Fig. S3 in Electronic Supplementary Material, the graphene nanosheets are highly interconnected, which could effectively impede the aggregation of VS_4 nanoparticles. Numerous nanosheets form porous 3D architectures which is similar to those previously reported for graphene aerogels [30,31]. Further investigations reveal that the nanorods are randomly coated on graphene nanosheets (Fig. 2(b) and Fig. S3(d) in Electronic Supplementary Material). Besides, abundant micropores can also be identified in those TEM images, which can be attributed to the water loss during the process of freeze-drying. As shown in Fig. 2(a), the building block contain wrinkles nanosheets having lateral sizes from 5 μm to tens of micrometers, and both sides of graphene are coated with nanorods which are about 5 nm in diameter. Figure 2(c) shows that a lattice periodicity of 0.56 nm is clearly observed by high-resolution TEM image, which can be attributed to the (110) planes of VS_4. Figure 2(d) displays the fast-Fourier transform (FFT), which further confirms the VS_4 phase of monoclinic.

Energy dispersive X-ray was used to demonstrate the

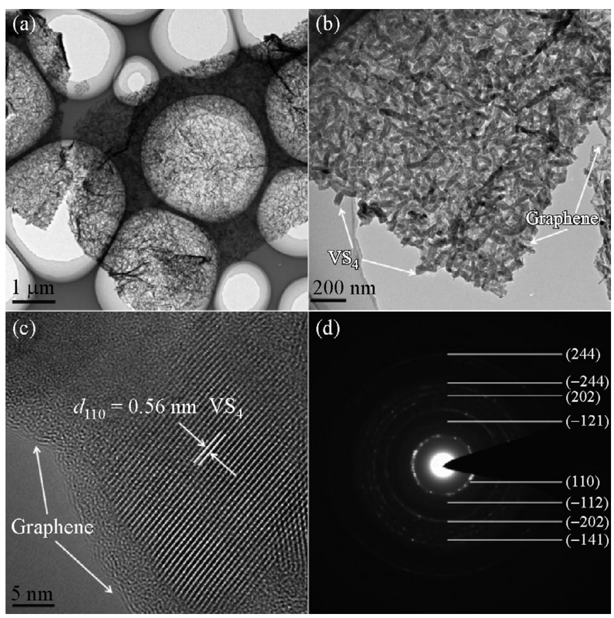

Fig. 2 TEM and HRTEM images of VS_4@GAs
(a) and (b) TEM images; (c) HRTEM images; (d) SAED pattern

composition of VS_4@GAs, and the elemental mapping analysis was used to show the distribution of elements (Fig. 3). The elemental atomic ratio of V and S is 1:4, and the V and S atoms are homogeneously distributed on the nanosheets. Figure S4 in Electronic Supplementary Material depicts the thermogravimetric curve of the VS_4@GAs with two steps of weight loss below 600°C. The first weight loss below 250°C is associated with the vanadium sulfide transfer to vanadium oxide, while the second weight loss can be attributed to the decomposition of the graphene in the temperature range of 300°C–500°C. The amount of graphene content in the composite is around 9.46 wt%.

The chemical composition of the VS_4@GAs was probed by using X-ray photoelectron spectroscopy (Fig. 4). As shown in Fig. 4(a), the characteristic peaks of C 1s, V 2p, and S 2p bands indicate the existence of C, S, and V. The C 1s spectra can be deconvoluted into three peaks of C-C, C-OH, and HO-C=O bonds respectively, indicating the formation of functional groups in graphene (Fig. 4(b)). The

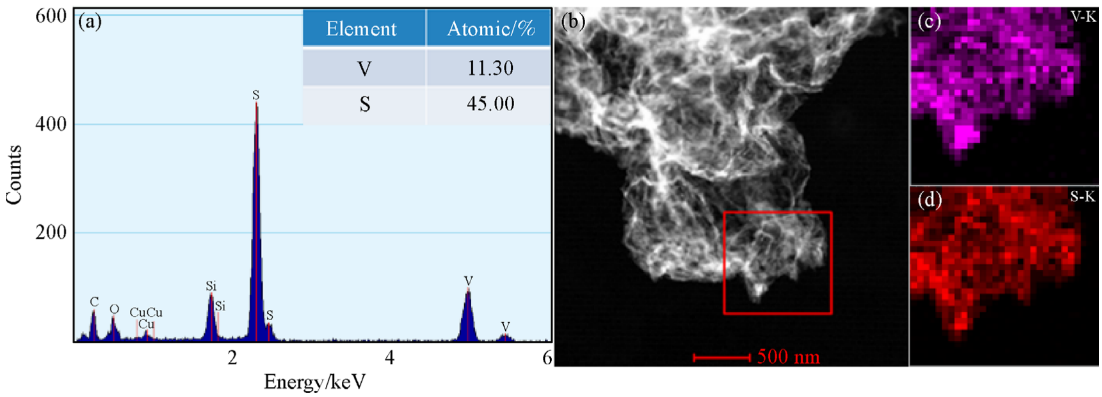

Fig. 3 Elemental distribution of VS_4@GAs
(a) EDS of VS_4@GAs; (b) SAED image; (c) elemental mapping image of V; (d) elemental mapping image of S

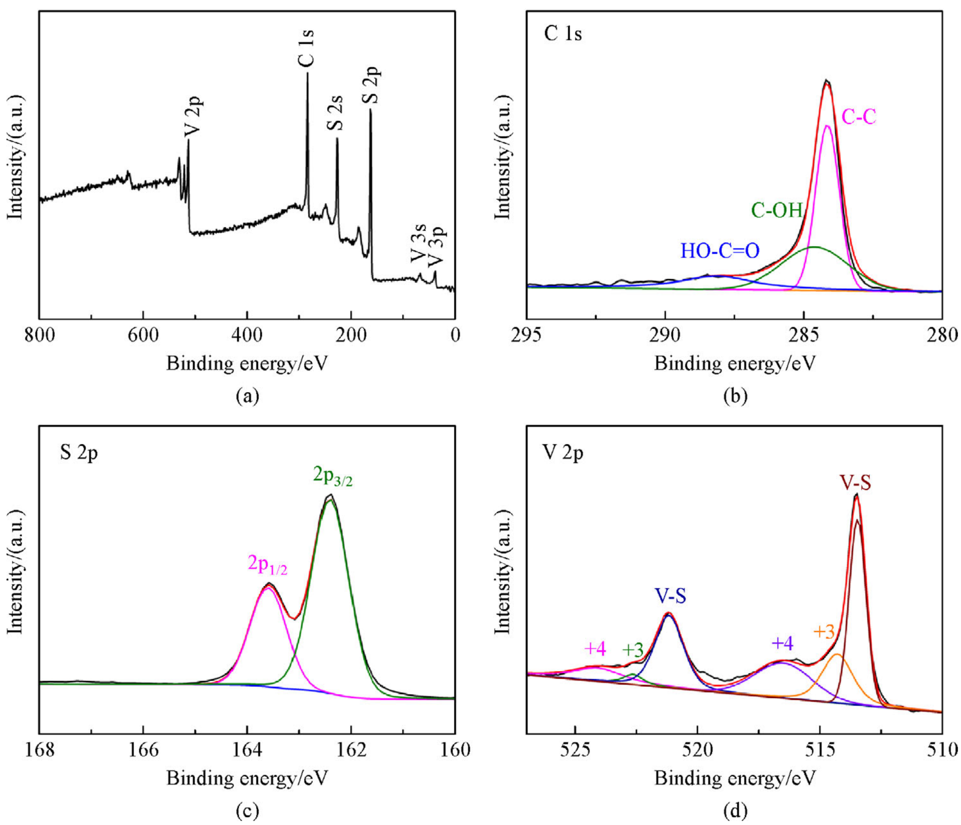

Fig. 4 XPS spectra of VS_4@GAs
(a) Survey spectrum; (b) C 1s; (c) S 2p; (d) V 2p

spectra of S 2p are constituted with peaks of $2p_{1/2}$ and $2p_{3/2}$ (Fig. 4(c)). In the spectra of V 2p (Fig. 4(d)), the peaks located at 513.5 eV and 521.2 eV can be ascribed to the bonds of V-S. On the other hand, the peaks located at 516.7 eV and 523.7 eV can be attributed to V^{4+}, while the small peak located at 514.7 eV arises from V^{3+}. This result indicates that the valence of V is mainly + 4, further confirming the formation of VS_4@GAs.

The electrochemical performance of VS_4@GAs composite as cathode material was tested. The cyclic voltammograms (CV) of VS_4@GAs tested at a scan rate of 0.2 mV/s in 1.5–3.0 V are shown in Fig. 5(a). During the initial cathodic scan, only one reduction peak located at 1.94 V appeared which could be ascribed to the lithium insertion VS_4 and the formation of Li_xVS_4 phase, corresponding to the equation: $x\mathrm{Li}^+ + \mathrm{VS}_4 + x\mathrm{e}^- \rightarrow \mathrm{Li}_x\mathrm{VS}_4$ ($x \leqslant 3$). Moreover, in the following anodic scan, two peaks of 2.29 V and 2.44 V were observed, which could be attributed to the multistep lithium extraction from the Li_xVS_4. Furthermore, all redox peaks show no obvious migration in subsequent cycles, indicating a good reaction reversibility upon lithiation and delithiation processes. Figure 5(b) displays the initial five galvanostatic charge-discharge profiles of the VS_4@GAs at a current density of 0.1 C (1 C = 400 mAh/g). The obviously discharge potential plateaus around 2.0 V can be assigned to the lithium ion intercalation into the VS_4, which is consistent with the CV results.

The rate capability of VS_4@GAs composite is illustrated at different current densities ranging from 0.1 to 5 C. (The specific capacity is calculated by the total mass of VS_4@GAs composite). As shown in Fig. 5(c), the VS_4@GAs electrode delivers a high specific capacity of 487, 443, 379, 326, and 244 mAh/g at a current density of 0.1, 0.2, 0.5, 1 and 2 C respectively. Moreover, even at a high rate of 5 C, the VS_4@GAs could still exhibit a discharge specific of 191 mAh/g. In addition, it is notable that all the discharge-charge curves at various current densities have similar discharge and charge plateaus, demonstrating the good rate capability of VS_4@GAs composite. Figure 5(d) displays the cycle performance of the VS_4@GAs electrode at 0.1C. The VS_4@GAs composite has a high discharge specific of 511 mAh/g and a charge specific capacity of 438 mAh/g, corresponding to an initial coulumbic efficiency (ICE) of 86%. The capacity loss can be attributed to the partially reversible lithium ion intercalation/extraction in VS_4. The VS_4@GAs could maintain a reversible capacity of 239 mAh/g after 15 cycles at a current density of 0.1 C. The obvious capacity decay of VS_4@GAs during the discharging/charging process further reveals that delithiation from Li_xVS_4 is much more difficult. Honestly, there is plenty of room to

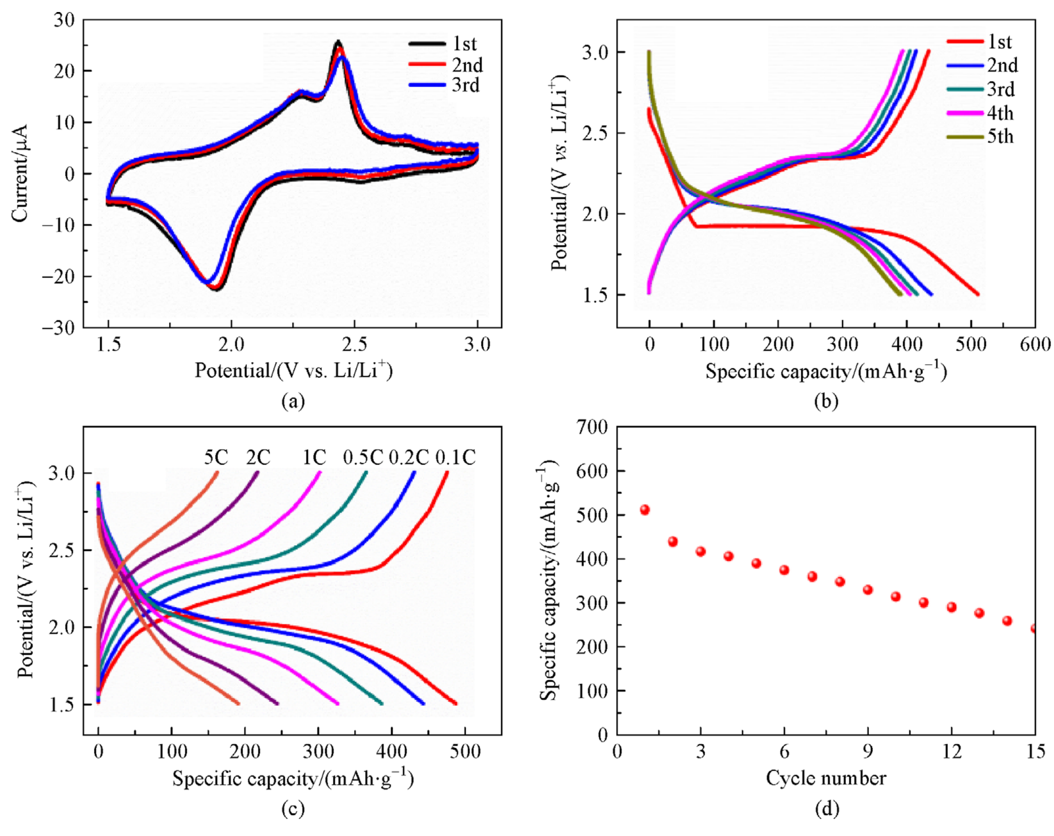

Fig. 5 Electrochemical performance of VS_4@GAs

(a) Cyclic voltammograms of VS_4@GAs at a scan rate of 0.2 mV/s; (b) discharge/charge curves of VS_4@GAs at a current density of 0.1 C; (c) charge/discharge capacities of VS_4@GAs at different current rates; (d) cycling performances of VS_4@GAs achieve high performance VS_4-baed cathode materials for LIBs by using more advanced nanostructure and composite methods.

3 Conclusions

In summary, VS_4@GAs was reported as a new cathode material for LIBs. The VS_4@GAs showed the mechanism of intercalations/deintercalations for lithium storage. Benefiting from the electron transfer highways in graphene and the abundant pores for Li^+ diffusion, the VS_4@GAs hybrid exhibits an enhanced cycle performance and rate capability. A high discharge capacity of 239 mAh/g can be remained after 15 cycles at a current density of 40 mA/g. Even at the high rate of 2000 mA/g, a discharge capacity of 191 mAh/g still can be obtained. The excellent electrochemical performance will provide new opportunities for the next-generation high-performance LIBs.

Acknowledgements This work was supported by the National Natural Science Foundation of China (Grant No. 21646012), the State Key Laboratory of Urban Water Resource and Environment, Harbin Institute of Technology (No. 2016DX08), China Postdoctoral Science Foundation (Nos. 2016M600253, and 2017T100246), the Postdoctoral Foundation of Heilongjiang Province, and the Fundamental Research Funds for the Central Universities (Grant No. HIT. NSRIF. 201836).

Electronic Supplementary Material Supplementary material is available in the online version of this article at http://dx.doi.org/10.1007/s11708-018-0576-9 and is accessible for authorized users.

References

1. Sun Y, Liu N, Cui Y. Promises and challenges of nanomaterials for lithium-based rechargeable batteries. Nature Energy, 2016, 1(7): 16071–16082
2. Li Y, Yao J, Uchaker E, et al. Leaf-like V_2O_5 nanosheets fabricated by a facile green approach as high energy cathode material for lithium-ion batteries. Advanced Energy Materials, 2013, 3(9): 1171–1175
3. Liu J, Zhou Y, Wang J, Pan Y, Xue D. Template-free solvothermal synthesis of yolk-shell V_2O_5 microspheres as cathode materials for Li-ion batteries. Chemical Communications (Cambridge), 2011, 47 (37): 10380–10382
4. Li B, Cheng Z, Zhang N, Sun K. Self-supported, binder-free 3D hierarchical iron fluoride flower-like array as high power cathode material for lithium batteries. Nano Energy, 2014, 4: 7–13
5. Li B, Zhang N, Sun K. Confined iron fluoride@CMK-3 nanocomposite as an ultrahigh rate capability cathode for Li-ion batteries. Small, 2014, 10(10): 2039–2046
6. Zhou Y, Liu P, Jiang F, Tian J, Cui H, Yang J. Vanadium sulfide submicrospheres: a new near-infrared-driven photocatalyst. Journal of Colloid and Interface Science, 2017, 498: 442–448
7. Zhang B, Zou S, Cai R, Li M, He Z. Highly-efficient photocatalytic disinfection of *Escherichia coli* under visible light using carbon supported Vanadium Tetrasulfide nanocomposites. Applied Catalysis B: Environmental, 2018, 224: 383–393
8. Das D P, Parida K M. Enhanced catalytic activity of Ti, V, Mn-grafted silica spheres towards epoxidation reaction. Catalysis Letters, 2009, 128(1–2): 111–118
9. Al-Shamma L, Naman S. Kinetic study for thermal production of hydrogen from H_2S by heterogeneous catalysis of vanadium sulfide in a flow system. International Journal of Hydrogen Energy, 1989, 14(3): 173–179
10. Jiang L, Lin B, Li X, et al. Monolayer MoS_2-graphene hybrid aerogels with controllable porosity for lithium-ion batteries with high reversible capacity. ACS Applied Materials & Interfaces, 2016, 8(4): 2680–2687
11. Tian R, Zhou Y, Duan H, et al. MOF-derived hollow Co_3S_4 quasi-polyhedron/MWCNT nanocomposites as electrodes for advanced lithium ion batteries and supercapacitors. ACS Applied Energy Materials, 2018, 1(2): 402–410
12. Zhu Y, Fan X, Suo L, Luo C, Gao T, Wang C. Electrospun FeS_2@carbon fiber electrode as a high energy density cathode for rechargeable lithium batteries. ACS Nano, 2016, 10(1): 1529–1538
13. Zhang Y, Wang N, Sun C, et al. 3D spongy CoS_2 nanoparticles/carbon composite as high-performance anode material for lithium/sodium ion batteries. Chemical Engineering Journal, 2018, 332: 370–376
14. Xu X, Jeong S, Rout C S, et al. Lithium reaction mechanism and high rate capability of VS_4–graphene nanocomposite as an anode material for lithium batteries. Journal of Materials Chemistry A, 2014, 2(28): 10847–10853
15. Lui G, Jiang G, Duan A, et al. Synthesis and characterization of template-free VS_4 nanostructured materials with potential application in photocatalysis. Industrial & Engineering Chemistry Research, 2015, 54(10): 2682–2689
16. Sun R, Wei Q, Li Q, et al. Vanadium sulfide on reduced graphene oxide layer as a promising anode for sodium ion battery. ACS Applied Materials & Interfaces, 2015, 7(37): 20902–20908
17. Liu P, Zhu K, Gao Y, et al. Recent progress in the applications of vanadium-based oxides on energy storage: from low-dimensional nanomaterials synthesis to 3D micro/nano-structures and free-standing electrodes fabrication. Advanced Energy Materials, 2017, 7 (23):
18. Su D, Wang G. Single-crystalline bilayered V_2O_5 nanobelts for high-capacity sodium-ion batteries. ACS Nano, 2013, 7(12): 11218–11226
19. Zhou Y, Tian J, Xu H, Yang J, Qian Y. VS_4 nanoparticles rooted by a-C coated MWCNTs as an advanced anode material in lithium ion batteries. Energy Storage Materials, 2017, 6: 149–156
20. Li Q, Chen Y, He J, Fu F, Lin J, Zhang W. Three-dimensional VS_4/graphene hierarchical architecture as high-capacity anode for lithium-ion batteries. Journal of Alloys and Compounds, 2016, 685: 294–299
21. Zhou Y, Li Y, Yang J, et al. Conductive polymer-coated VS_4 submicrospheres as advanced electrode materials in lithium-ion batteries. ACS Applied Materials & Interfaces, 2016, 8(29): 18797–18805
22. Cheng J, Gu G, Guan Q, et al. Synthesis of a porous sheet-like V_2O_5-CNT nanocomposite using an ice-templating 'bricks-and-

mortar'assembly approach as a high-capacity, long cyclelife cathode material for lithium-ion batteries. Journal of Materials Chemistry, 2016, 4(7): 2729–2737

23. Yang Y, Huang J, Zeng J, Xiong J, Zhao J. Direct electrophoretic deposition of binder-free Co_3O_4/graphene sandwich-like hybrid electrode as remarkable lithium ion battery anode. ACS Applied Materials & Interfaces, 2017, 9(38): 32801–32811
24. Chen D, Ji G, Ma Y, Lee J Y, Lu J. Graphene-encapsulated hollow Fe_3O_4 nanoparticle aggregates as a high-performance anode material for lithium ion batteries. ACS Applied Materials & Interfaces, 2011, 3(8): 3078–3083
25. Li B, Rooney D W, Zhang N, Sun K. An *in situ* ionic-liquid-assisted synthetic approach to iron fluoride/graphene hybrid nanostructures as superior cathode materials for lithium ion batteries. ACS Applied Materials & Interfaces, 2013, 5(11): 5057–5063
26. Fan L, Li B, Rooney D W, Zhang N, Sun K. *In situ* preparation of 3D graphene aerogels@hierarchical Fe_3O_4 nanoclusters as high rate and long cycle anode materials for lithium ion batteries. Chemical Communications (Cambridge), 2015, 51(9): 1597–1600
27. Cheng G, Akhtar M S, Yang O B, Stadler F J. Novel preparation of anatase TiO_2@reduced graphene oxide hybrids for high-performance dye-sensitized solar cells. ACS Applied Materials & Interfaces, 2013, 5(14): 6635–6642
28. Fan L, Zhang Y, Zhang Q, Wu X, Cheng J, Zhang N, Feng Y, Sun K. Graphene aerogels with anchored sub-micrometer mulberry-like ZnO particles for high-rate and long-cycle anode materials in lithium ion batteries. Small, 2016, 12(37): 5208–5216
29. Xiao J, Mei D, Li X, et al. Hierarchically porous graphene as a lithium–air battery electrode. Nano Letters, 2011, 11(11): 5071–5078
30. Xiao L, Wu D, Han S, et al. Self-assembled Fe_2O_3/graphene aerogel with high lithium storage performance. ACS Applied Materials & Interfaces, 2013, 5(9): 3764–3769
31. Fang W, Zhang N, Fan L, Sun K. Bi_2O_3 nanoparticles encapsulated by three-dimensional porous nitrogen-doped graphene for high-rate lithium ion batteries. Journal of Power Sources, 2016, 333: 30–36